SAND2015-2089C

Application of Equalization Notch to Improve Synthetic Aperture Radar Coherent Data Products

Cameron Musgrove[a] and James C. West[b]

[a]Sandia National Laboratories, PO Box 5800, Albuquerque, NM 87185;
[b]Oklahoma State University, 202 Engineering South, Stillwater, OK 74078.

ABSTRACT

Interference and interference mitigation techniques degrade synthetic aperture radar (SAR) coherent data products. Radars utilizing stretch processing present a unique challenge for many mitigation techniques because the interference signal itself is modified through stretch processing from its original signal characteristics. Many sources of interference, including constant tones, are only present within the fast-time sample data for a limited number of samples, depending on the radar and interference bandwidth. Adaptive filtering algorithms to estimate and remove the interference signal that rely upon assuming stationary interference signal characteristics can be ineffective. An effective mitigation method, called notching, forces the value of the data samples containing interference to zero. However, as the number of interference sources increase and the number of data samples set to zero increases, image distortion and loss of resolution degrade both the image product and coherent data products.

Techniques to repair image distortions,[1] are effective for point-like targets. However, these techniques are not designed to model and repair distortions in SAR image terrain. Good terrain coherence is important for SAR second order image products because terrain occupies the majority of many scenes. For the case of coherent change detection it is the terrain coherence itself that determines the quality of the change detection image.

This paper proposes an unique equalization technique that improves coherence over existing notching and equalization techniques. First, the proposed algorithm limits mitigation to only the samples containing interference, unlike adaptive filtering algorithms, so the remaining samples are not modified. Additionally, the mitigation adapts to changing interference power such that the resulting correction equalizes the power across the data samples. The result is reduced distortion and improved coherence for the terrain. Real SAR data demonstrates improved coherence from the proposed equalization correction over existing notching methods for chirped interference sources.

Keywords: synthetic aperture radar, interference mitigation, coherent change detection

1. INTRODUCTION

In the future, it is expected wireless communication systems will require more bandwidth to support an increasing need for greater data throughput from growing consumer demand. A prime example is cellular telephone providers desire more bandwidth to increase the number of users and increase the amount of data that can be transmitted on their networks.[2] The amount of bandwidth a communication provider can use is limited to the spectrum allocation policies made by government entities, such as the NTIA in the United States. Researchers are examining higher frequencies outside of what is considered to be traditional cellular telephone communication spectrum, in particular 28GHz,[2] and including parts of the spectrum where military radar systems operate. In response to the public need for more spectrum, the United States' Department of Defense (DoD) is finding ways to allocate more spectrum to commercial use.[3] The DoD is pursuing a broad strategy that includes coordination, sharing, and co-operation.[4] The reality is that in the future there will be a greater number of systems trying to use the same spectrum of frequencies. It is inevitable that two different radar systems will have to operate in the same area within the same frequency band.

This paper considers the case where additional, unwanted signal energy from another radar system is received by a synthetic aperture radar. There are many examples of interference effects upon synthetic aperture radar (SAR) images in

Further author information: (Send correspondence to C.M.)
C.M.: E-mail: cmusgro@sandia.gov
J.W.: E-mail: jwest@okstate.edu

the literature, and associated mitigation techniques.[5–9] Many interference mitigation techniques are tuned to a particular type of interference for a specific radar. Although most of these techniques are not designed to mitigate chirped sources of interference, many of the techniques could be applicable. For many SAR systems mitigating interference artifacts from imagery is not the only concern, maintaining the quality of second order products, such as interferometric SAR (IFSAR) and coherent change detection (CCD), is important. For these SAR systems the chosen interference mitigation must also restore the quality of the second order products to be considered successful.

This paper presents a study of the quality of both the SAR image and second order data products in response to interference from a chirped signal and the effects from mitigating the chirped signal interference. First, background is presented on interference effects, interference detection, and previous approaches. It is shown that attempts to repair interference mitigation distortions from notching[8] are not designed for general terrain image features. To reduce the distortion to the image, a new approach to notching data is presented, called equalization notch. Finally, real SAR data is used to validate the improvement in image quality and average coherence from using the new equalization notch technique over a standard notching technique for a couple of examples.

2. BACKGROUND

The SAR system modeled for this paper (and used for data collection) utilizes deramp processing. Essentially, deramp processing limits range swath to reduce the A/D sampling requirements; more details on deramp processing can readily be found in the literature.[10–12] For any signal received by the radar, including interference, deramp processing mixes a chirp with that signal, thereby changing the interference signal parameters. For a constant tone interference source, the result is a chirped tone time-limited within the SAR phase history data samples. This is in contrast to a direct-sample SAR where the constant tone interference signal exists in all SAR phase history data samples as a constant tone. This means the sampling architecture of the radar alone can decide what class of mitigation algorithms are applicable to mitigate the interference. For example, for direct-sample SAR systems adaptive filters[13,14] and frequency notching[9] can be quite effective. However, the non-stationary characteristic of the interference in the deramp phase history makes it difficult to apply adaptive filtering techniques because adaptive filters have an adjustment period. Frequency notching can be more damaging to deramp SAR image quality because the residual chirp on the interference signal can spread its energy across many more frequencies than the interference source bandwidth. It should be noted that it is possible to remove the residual chirp spreading effect upon a constant tone interference signal by deskew processing,[8,15] however this is only effective if the signal is a constant tone or very small bandwidth. If the signal is not a constant tone, in certain cases, the deskew correction can actually increase the number of samples occupied by the interference energy.

2.1 Interference Model

The chirped interference signal is modeled as a linear frequency-modulated chirp in the form

$$A_i(t) = A \exp j \left\{ \omega_i t + \frac{\gamma_i}{2} t^2 \right\}, \tag{1}$$

where ω_i is the center frequency, γ_i is the chirp rate, A is the amplitude, and t is time. Additionally, the chirped interference source has its own duty factor and pulse repetition frequency (PRF) separate from the SAR.

Interference affects SAR images by creating additional shapes, patterns, or smears, called artifacts, within the image. Fig. 1 gives an example of a SAR image without interference and an image with interference; the effect of the interference is clear. Fig. 1 is a 6 inch range and cross-range resolution image collected by Sandia National Laboratories Ku-band SAR testbed platform.

For second order products, like IFSAR and CCD, interference artifacts can be very damaging. The quality of IFSAR and CCD products depend upon maximizing coherence between the two images.[16,17] For this paper, coherence is measured between two identical data collections, or passes, recorded at different times from the same location in space. The true coherence, like the mean value of a population, can only be estimated from the image data. The performance of the estimator can vary under certain conditions,[17] and there are a few different estimators available to choose.[17,18] The estimator used in this paper is the maximum likelihood estimator[16,17,19] of coherence defined as

$$\hat{\mu} = \frac{\sum_{n=1}^{L-1} x_{1,n} x_{2,n}^*}{\sqrt{\sum_{n=1}^{L-1} |x_{1,n}|^2 \sum_{n=1}^{L-1} |x_{2,n}|^2}}, \tag{2}$$

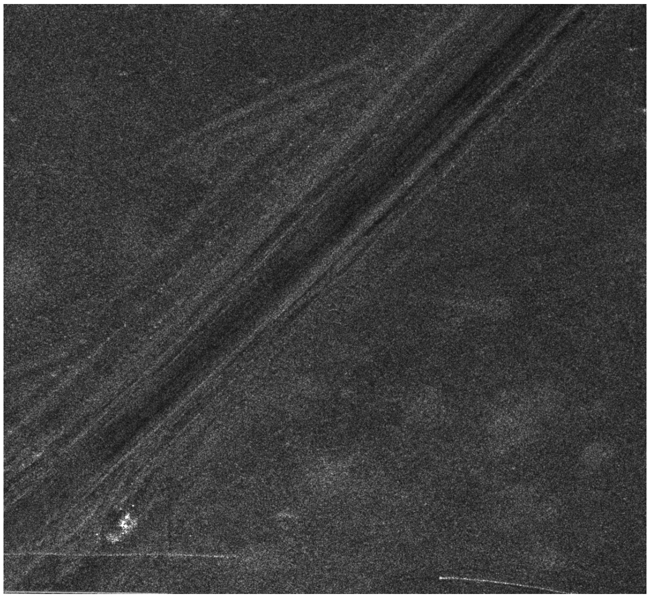

(a) SAR image

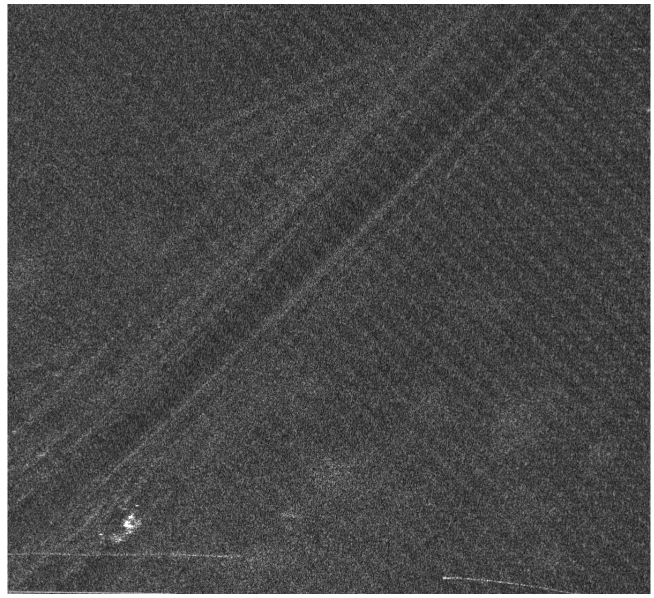

(b) SAR image with interference

Figure 1: Comparison of a typical SAR image (a) without interference and (b) with interference. Interference source is 300MHz chirp centered at 16.8GHz with PRF 10Hz and duty factor of 20% at signal to interference power ratio of -5dB.

where L is the number of 'looks' or local pixels, $x_{1,n}$ is the nth pixel of image 1, and $x_{2,n}$ is the nth pixel of image 2. The magnitude of coherence, $|\hat{\mu}|$, is displayed as a CCD image, whereas the phase of coherence, $\angle\hat{\mu}$ can be processed into a height map. The values of the coherence are limited to the interval $[0,1]$. To quantitatively evaluate the quality of a CCD, a common metric is to compute the average magnitude of coherence for all the pixels in the image. The higher the average, the better the match between the two images. A value of 1 indicates an exact match between images. The CCD image is created when the values of coherence are mapped to a color map. A gray-scale color map is used in this paper and assigns a coherence value of zero to black and a coherence value of 1 to white. The specific target and radar parameters determine acceptable coherence limits for a system.

There are many sources in the literature that discuss the loss mechanisms that define the maximum achievable coherence value between two images.[16,17,20–22] These loss mechamisms are multiplicative, cascading as

$$\mu = \mu_{SNR} \cdot \mu_{temporal} \cdots \tag{3}$$

Within this paper the loss factor of primary concern is coherence loss due to signal-to-noise ratio (SNR).

Unmitigated, the interference artifacts contribute to the noise power in the SNR calculation, because the interference is not the signal of interest. In the presence of interference it is common to use the term signal to interference plus noise ratio (SINR). The relationship between coherence and SNR or SINR is

$$\mu_{SNR} = \frac{SINR}{SINR+1}. \tag{4}$$

An example of a CCD with high coherence values and without interference in either pass is found in Fig. 2a. In Fig. 2b the interference in the SAR image in Fig. 1b generally lowers the coherence values, so the CCD image appears darker.

2.2 Detector

The detector used in this paper is a power detector based upon the detector in Wahl et. al.[8] except this detector uses a priori knowledge of the interference source bandwidth to estimate the mean and standard deviation of the magnitude data values from the data itself to set a detection threshold. The details of this detector are described below along with a block diagram in Fig. 3.

(a) SAR CCD (b) SAR CCD with interference

Figure 2: Comparison of a typical SAR CCD image (a) without interference and (b) with interference. Interference source is 300MHz chirp centered at 16.8GHz with PRF 10Hz and duty factor of 20% at signal to interference power ratio of -5dB.

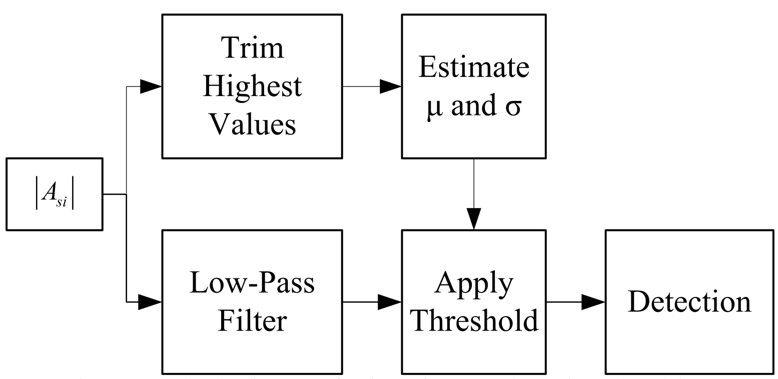

Figure 3: Block diagram for interference detection algorithm.

Figure 4: Comparison of the SAR image effects with notching (a) 5% of data samples and (b) 25% of data samples. Assuming ideal interference detection.

On a pulse by pulse basis, mean and standard deviation values are estimated directly from trimmed magnitude values of the phase history signal plus interference, $|A_{si}|$. Meyer[5] shows how trimming data can be effective to estimate statistics of radar data containing interference. However, unlike a typical trim operation that is double sided, the trim operation for this detector only removes the largest data values because the magnitude phase history data approximates a Rayleigh distribution. If the interference energy is larger than the target return energy, then the single sided trim can result in a lower bias for the estimated mean value.

Once the mean and standard deviation values of the data are estimated a threshold value can be calculated. The threshold is applied to low-pass filtered phase history magnitude data to reduce the false alarms throughout the phase history and reduce missed detections within the interference bandwidth.[8]

2.3 Typical Approach to Interference Mitigation

A typical approach to mitigate interference energy, particularly when the radar bandwidth exceeds the interference signal bandwidth, is to simply remove (or notch) the spectrum containing interference energy.[5,7,8,23] While effective at removing interference artifacts from SAR imagery, this mitigation corrupts the impulse response (IPR) of the radar image. The amount of IPR distortion depends on where and how much spectrum is notched,[24] and generally increases as the number of samples or percent of spectrum notched increases. To observe the results of the mitigation itself, in particular the notch mitigation, we will consider a few cases with an ideal detector so that any and all IPR distortions are due solely to the mitigation technique. Fig. 4 illustrates the effect notching can have on a SAR image for small and large notches. Fig. 5a shows notching only 5% of data samples results in a small but noticeable amount of image distortion. The point-like reflectors in the lower-left of Fig. 5a show the IPR distortion as vertical streaks. When 25% of samples are notched, as shown in Fig. 5b, the clutter/terrain IPR distortion begins to blur details throughout the image. For example the road is lighter in color and not as distinct, particularly when compared to Fig. 1a.

IPR distortion can be devastating to second order products, like CCD. IPR distortion is characterized by higher sidelobe levels than the ideal IPR, which induce a correlation between adjacent pixels.[17] The increased sidelobe energy, once in neighboring pixels, can either create false changes or mask true changes.[17] Fig. 5 shows the resulting CCD products for the above notched images in Fig. 4 when computed against a reference image without distortions.

To remove IPR distortions from notching, Wahl et. al.[8] showed that the CLEAN[1] algorithm can repair distortions for point-like responses. Essentially, CLEAN uses a model of the distorted point target IPR to remove the distorted point target from the image and then replace it with an idealized IPR.[1] Unfortunately, CLEAN is not designed to model SAR clutter (terrain) response, so the clutter IPR remains distorted and contributes to the degradation of the second order products. Fig. 6 shows the image from Fig. 5b repaired with CLEAN and the associated CCD remains the same as Fig. 5d; notice the point targets in the lower left corner no longer have high sidelobes (vertical streaking) but the overall terrain coherence is the same.

Fig. 7 shows a single pulse phase history after applying the standard notch corresponding to the image in Fig. 5b and CCD in Fig. 5d. The advantage of the standard notch is that if the detector is able to identify all the samples containing interference, then the standard notch eliminates all interference energy. However, excising the data samples leaves magnitude and phase discontinuities in the phase history signal. If the data signal follows an ideal model of a point target, CLEAN is able to repair these discontinuities, but the random nature of the clutter signal makes it difficult to fit a model. Therefore this paper seeks an alternative to notching that removes interference and lessens damage to the clutter IPR and increases overall image coherence. The following section describes a mitigation technique that satisfies these goals under certain conditions.

3. EQUALIZATION NOTCH MITIGATION TECHNIQUE

The equalization notch mitigation algorithm equalizes the magnitude of the phase history data samples containing interference to the level of the data samples without interference. Only the samples detected as containing interference are

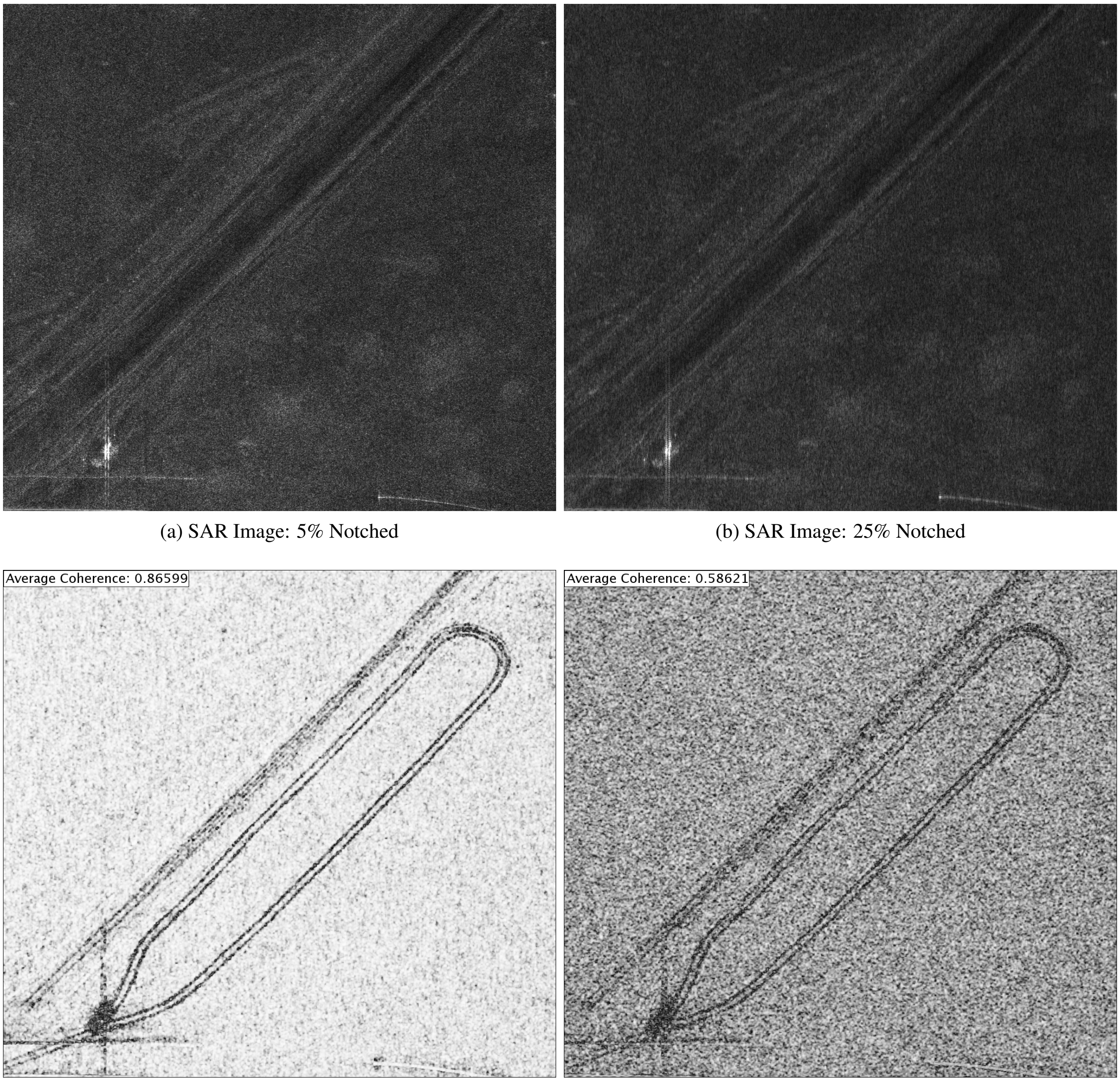

(a) SAR Image: 5% Notched

(b) SAR Image: 25% Notched

(c) CCD Image: 5% Notched

(d) CCD Image: 25% Notched

Figure 5: Comparison of the image effects due to notching. Ideal interference detection is assumed in these examples.

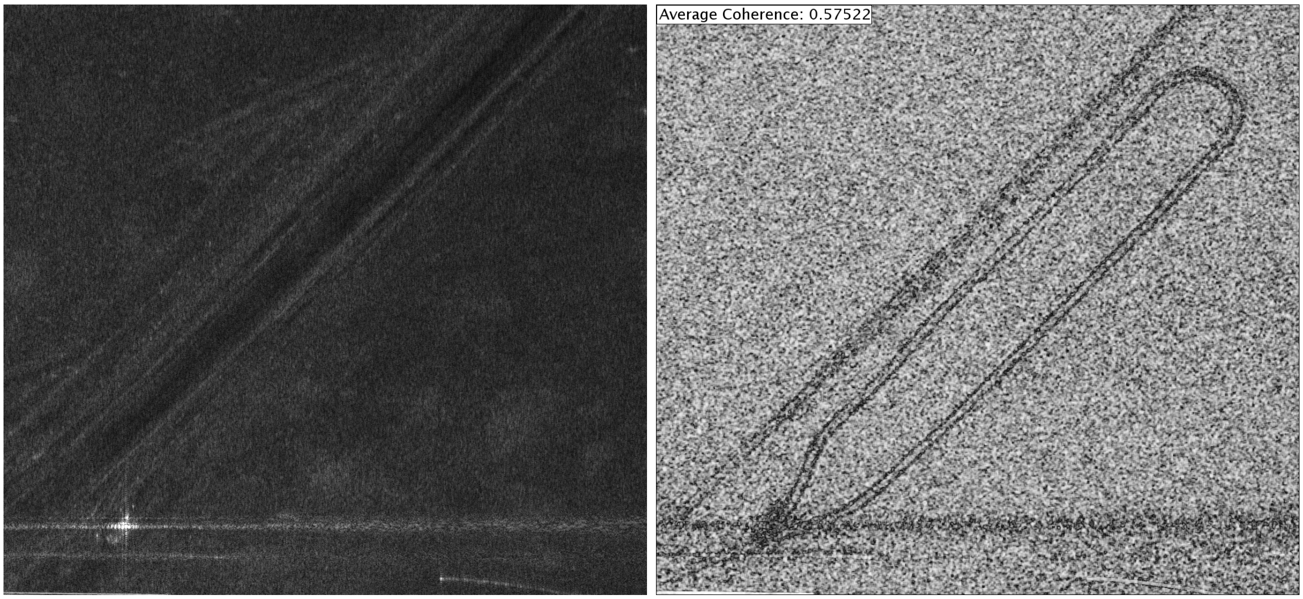

(a) SAR Image: 25% Notched, CLEAN Applied (b) CCD Image: 25% Notched, CLEAN Applied

Figure 6: Example of using CLEAN after notching 25% of data samples for (a) the SAR image and (b) CCD image. Assuming an ideal interference detector.

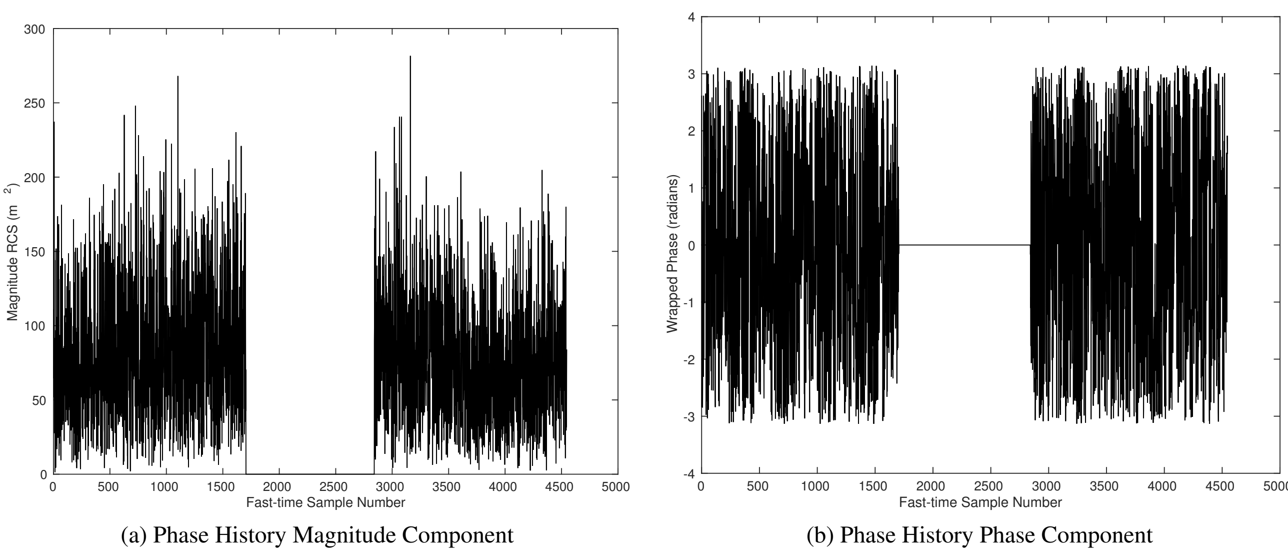

(a) Phase History Magnitude Component (b) Phase History Phase Component

Figure 7: Magnitude and phase components of a single pulse's phase history with 25% of data samples notched to show the signal discontinuities from applying a notch.

modified, but interference is not completely eliminated as is the case with notching. In effect, the energy from the interference signal is reduced so its image artifacts are less apparent in the final image. Furthermore, only the magnitude is adjusted while the phase remains unchanged.

The concept is to adjust the phase history magnitude to be relatively flat across fast-time samples within a single pulse because an ideal phase history magnitude is relatively flat across all data samples. This is because the radar samples a tone, representing the target response, with a finite number of samples. The result of digital sampling of a tone can be considered a multiplication of a rectangular window function and the tone. Any changes to the magnitude of the rectangular function can also be considered the product of a weighting function. Typical SAR processors apply a weighting function to control sidelobes,[11,19] but if the weighting function is not of a particular shape or value to reduce sidelobes, like the case where data samples are notched, the weighting can actually increase the sidelobe level. Therefore, one approach to repairing an IPR is to equalize the phase history data such that it closely resembles the rectangular function (or desired window function) necessary for the ideal IPR. In the case of interference, equalizing the interference values to the non-interference values can reduce the amplitude of image artifacts and reduce IPR distortion.

The equalization notch algorithm is implemented as a sample-varying weighting vector, k, that varies according to each data sample's magnitude value and the measured mean of the phase history data, $\hat{\mu}_s$. To calculate the weighting vector, first assume the resulting magnitude of the equalized phase history, $|A_{en}|$ can be expressed as the function of a weighting vector and the phase history data containing signal and interference, $|A_{si}|$, or

$$|A_{en}| = k|A_{si}|. \tag{5}$$

And assume that $|A_{en}|$ represents the original data minus the interference magnitude, $|A_i|$, or

$$|A_{en}| = |A_{si}| - |A_i|. \tag{6}$$

Since $|A_i|$ is not known, it can be estimated by calculating an envelope of the original magnitude data, $|\tilde{A}_{si}|$ and subtracting the estimated mean value of the data without interference, $\hat{\mu}_s$. The envelope, $|\tilde{A}_{si}|$ can be calculated with a median filter; practically a small filter size works well. If the filter is too large, then short duration interference is not suppressed. But, if the filter is too small then too much energy is suppressed.

Using the above relations, the filter weights can be calculated as

$$\begin{aligned} k|A_{si}| &= |A_{si}| - |A_i|, \\ k|A_{si}| &= |A_{si}| - \left(|\tilde{A}_{si}| - \hat{\mu}_s\right), \\ k &= 1 - \frac{\left(|\tilde{A}_{si}| - \hat{\mu}_s\right)}{|A_{si}|}. \end{aligned} \tag{7}$$

Next, the interference detector determines which sample indices contain interference and only applies the weighting to the corresponding indices identified to contain interference. The estimate of the mean magnitude value, $\hat{\mu}_s$ is calculated by the detector described earlier in this paper using trimmed data values.

As the energy of the interference signal increases, the performance of the equalization notch algorithm will theoretically degrade below that of the standard notch because the phase component of the interference remains un-mitigated. It turns out there is a particular range of signal-to-interference ratio (SIR) values where the interference distortion from the phase component is less than the distortion from notching the data values to zero.

4. REAL DATA EXAMPLES

Real SAR data of terrain, with real changes, for two collection scenarios are used to demonstrate coherence improvement predicted by simulations. Unfortunately, SAR data with chirped interference sources is not available at this time, therefore a chirped interference source is synthetically added to one data set to create the first scenario. The second scenario uses data that contains a constant tone interference source. The constant tone can approximate a chirp signal because the deramp processing adds a chirp to the constant tone interference. In both scenarios, the first image is clear of any interference while the second image for the CCD contains interference. Again, this is done so that the image quality and CCD quality are measured together by the average coherence value. Furthermore, these data examples also evaluate both the effectiveness of the detector described earlier and the mitigation method. The coherence values in these real data examples will be lower in comparison to Fig. 5 due to interference artifacts of the interference energy missed by the detector. Although the detector is not perfect, the results are comparable between mitigation methods because both methods use the same detector.

The first scenario shows the effect of a synthetically created 300MHz chirped bandwidth interference source centered at 16.8GHz with a PRF of 10Hz, duty factor of 20%, and SIR of -10dB upon a SAR image in Fig. 8a and the associated CCD image in Fig. 8b. The addition of image artifacts from the interference source nearly decorrelates the scene. Fig. 8c shows the resulting CCD from applying the standard notch and CLEAN has improved the coherence, however the overall coherence is still lower than a CCD produced after using the equalization notch mitigation in Fig. 8d. For this scenario, the amount of samples detected to contain interference varies depending upon the pulse length and duty factor of the interference therefore not all pulses contain interference energy. During interference transmission 22.8% of fast-time samples are identified to contain interference. Due to the one-sided trimming, when no interference is transmitted during the SAR pulse 13% of fast-time samples are identified as containing interference. Overall, the amount of samples notched in this scenario is less than 25% and the average coherence is higher than the ideal detector results for Fig. 5d and Fig. 6b despite any interference energy missed by detector and coherence losses due to processing real data (e.g. registration, phase errors, etc.).

In the second scenario, a SAR image with a 16.7GHz constant tone at SIR of -4 dB is shown in Fig. 9a and its associated CCD in Fig. 9b. Again, this data set emulates a chirped interference source by using the radar's deramp processing to chirp the constant tone interference source. But unlike scenario 1, the interference source energy is present in every pulse. The detector identifies approximately 22% of fast-time samples as containing interference. Like scenario one, Fig. 9c and Fig. 9d demonstrate the equalization notch provides an average coherence improvement over the standard notch and CLEAN algorithm.

5. CONCLUSIONS

This paper examines a possible scenario where another radar system is using the same spectrum in the same place as a SAR. Despite the interference energy from the other radar system, the SAR needs to maintain both image quality and second order products specifications, such as IFSAR and CCD. A new interference mitigation method is introduced that reduces IPR distortion and increases average coherence over a notching approach. The coherence improvement of the equalization notch over a notch technique has been validated with real SAR data.

While the goal of this work was to improve quality for both images and second order products, it has been shown that coherence can be a powerful metric to compare relative performance between different interference mitigation methods. Coherence has been used in the past[7] to tune an adaptive filter, but not as a relative performance measure against alternate mitigation techniques. In the way it is used in this paper, coherence quantitatively measures image quality because the first image is undisturbed by interference or mitigation. However, if both images had an identical, but poor IPR, then coherence would be high and no longer indicative of image quality. Ultimately for a CCD product, it is the probability of detecting a real change that is the most important. Future work should quantify the performance of an interference mitigation technique to the probability of detecting change.

The effectiveness of the methods presented in this paper, like other interference mitigation methods, have a limited region of usefulness. For certain cases where interference is very narrowband, notching can be an excellent mitigation method. However, as interference bandwidth increases, other methods, like equalization or equalization notch, may provide a coherence performance increase. But even these methods have limits. In the end it is up to the radar system designer to determine the mitigation algorithm trade-offs necessary for the radar system to meet is goals.

ACKNOWLEDGMENTS

Author C.M. would like to thank Richard Ormesher, Bill Hensley, Jason Payne, and Rusty Escapule for their support in pursuing this work, and Richard Naething and Derek Tucker for productive technical discussions.

Sandia National Laboratories is a multi-program laboratory managed and operated by Sandia Corporation, a wholly owned subsidiary of Lockheed Martin Corporation, for the U.S. Department of Energy's National Nuclear Security Administration under contract DE-AC04-94AL85000.

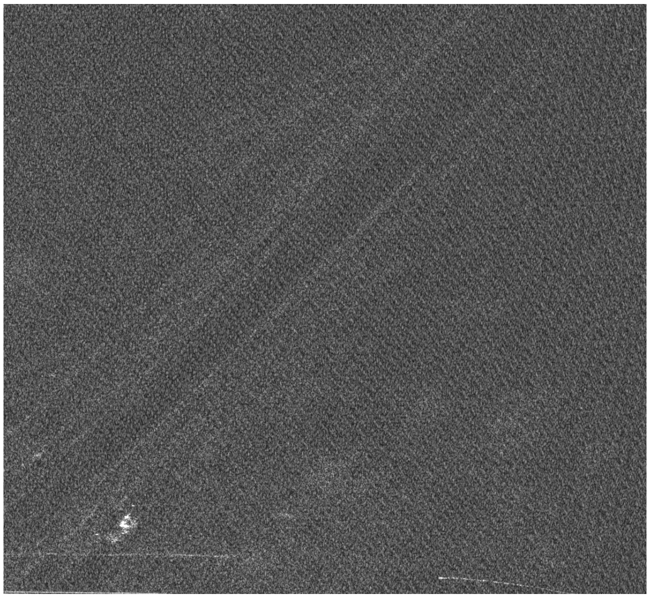

(a) SAR Image With Interference

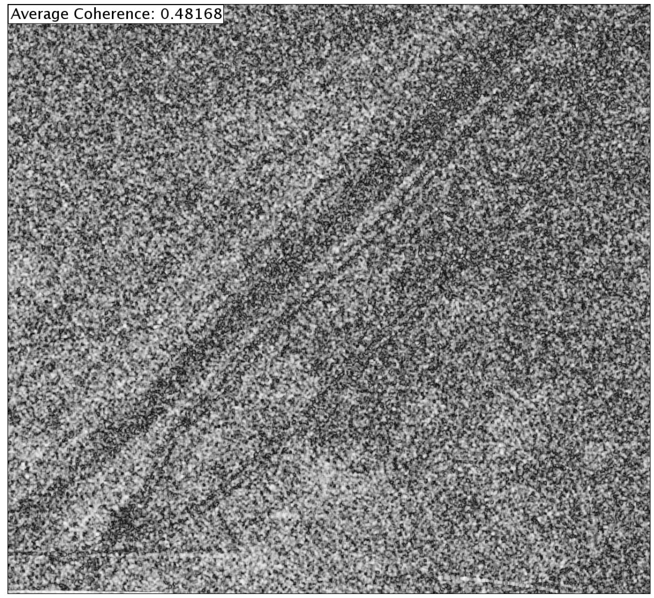

(b) CCD Image With Interference

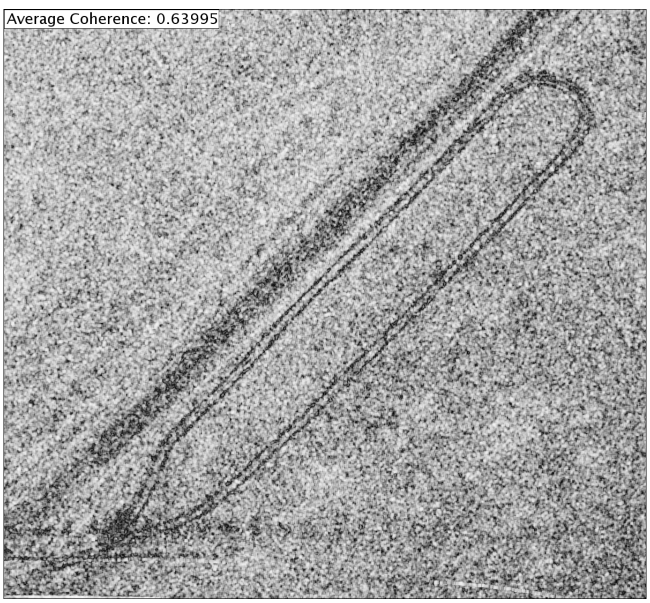

(c) CCD After Mitigation with Notch and CLEAN

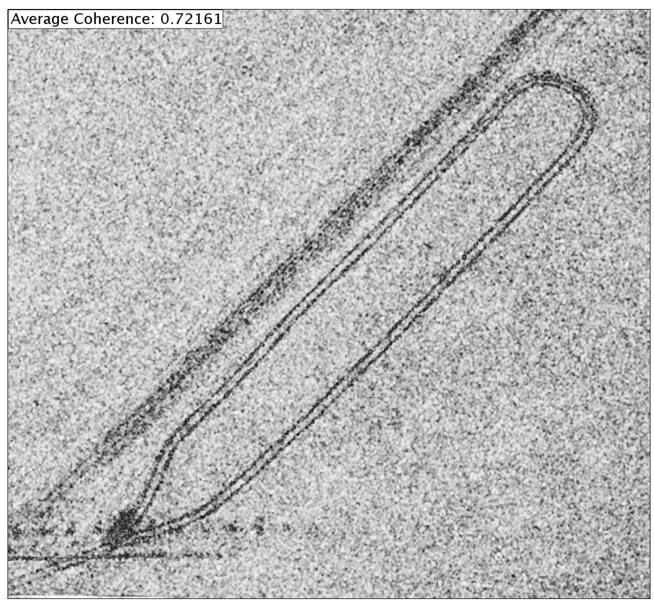

(d) CCD After Mitigation with Equalization Notch

Figure 8: Real data example to demonstrate effectiveness of mitigation technique upon the CCD product. This case is for a synthetically generated 300MHz chirped bandwidth interference source centered at 16.8GHz with a PRF of 10Hz, duty factor of 20%, and SIR of -10dB. (a) a SAR image corrupted with synthetic interference, (b) CCD image corrupted with synthetic interference, (c) CCD product after applying notch and CLEAN algorithms, and (d) CCD product of the two images after applying the equalization notch.

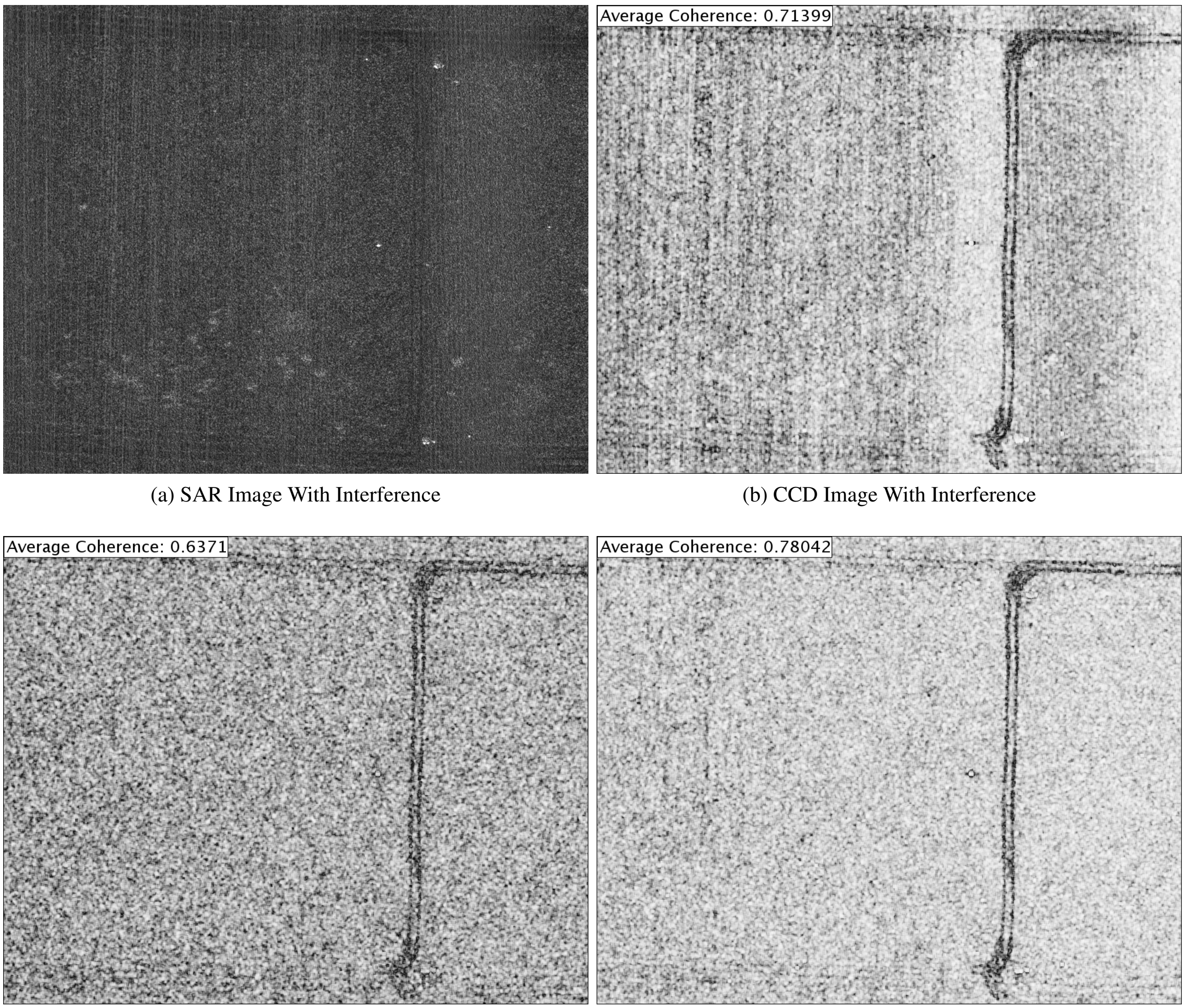

(a) SAR Image With Interference

(b) CCD Image With Interference

(c) CCD After Mitigation with Notch and CLEAN

(d) CCD After Mitigation with Equalization Notch

Figure 9: Real data example to demonstrate effectiveness of mitigation technique upon the CCD product. This case uses a constant 16.7GHz tone as the interference source, without deskew processing at a SIR of -4dB. (a) a SAR image corrupted with synthetic interference, (b) CCD image corrupted with synthetic interference, (c) CCD product after applying notch and CLEAN algorithms, and (d) CCD product of the two images after applying the equalization notch.

REFERENCES

[1] Tsao, J. and Steinberg, B., "Reduction of sidelobe and speckle artifacts in microwave imaging: the CLEAN technique," *IEEE Transactions on Antennas and Propagation* **36**, 543–556 (Apr. 1988).

[2] Rappaport, T., Roh, W., and Cheun, K., "Mobile's millimeter-wave makeover," *IEEE Spectrum* **51**, 34–58 (Sept. 2014).

[3] "DoD Releases Electromagnetic Spectrum Strategy," (Feb. 2014).

[4] "Electromagnetic Spectrum Strategy," tech. rep. (2013).

[5] Meyer, F., Nicoll, J., and Doulgeris, A., "Correction and Characterization of Radio Frequency Interference Signatures in L-Band Synthetic Aperture Radar Data," *IEEE Transactions on Geoscience and Remote Sensing* **51**(10), 4961–4972 (2013).

[6] Lamont-Smith, T., Hill, R. D., Hayward, S. D., Yates, G., and Blake, A., "Filtering approaches for interference suppression in low-frequency SAR," *Radar, Sonar and Navigation, IEE Proceedings -* **153**, 338–344 (Aug. 2006).

[7] Reigber, A. and Ulbricht, A., "P-band repeat-pass interferometry with the DLR experimental SAR (ESAR): first results," in [*Geoscience and Remote Sensing Symposium Proceedings, 1998. IGARSS '98. 1998 IEEE International*], **4**, 1914–1916 vol.4 (1998).

[8] Wahl, D., Yocky, D. A., Jakowatz, C. V., Thompson, P., Erteza, I., and Doren, N., "Interesting Aspects of Spotlight-Mode Image Formation for an L/S-Band High-Resolution SAR," in [*Proceedings of the Workshop on Synthetic Aperture Radar Technology*], (2002).

[9] Ulander, L. M. H. and Forlind, P.-O., "Precision processing of CARABAS HF/VHF-band SAR data," in [*Geoscience and Remote Sensing Symposium, 1999. IGARSS '99 Proceedings. IEEE 1999 International*], **1**, 47–49 vol.1 (1999).

[10] Richards, M. A., [*Fundamentals of Radar Signal Processing*], McGraw Hill Professional (June 2005).

[11] Carrara, W. G., Goodman, R. S., and Majewski, R. M., [*Spotlight Synthetic Aperture Radar: Signal Processing Algorithms*], Artech House, Incorporated (Jan. 1995).

[12] Doerry, A. W., "Wavefront curvature limitations and compensation to polar format processing for synthetic aperture radar images," tech. rep., Sandia National Laboratories (2007).

[13] Vu, V.-T., Sjogren, T., Pettersson, M., Hkansson, L., Gustavsson, A., and Ulander, L. M. H., "RFI Suppression in Ultrawideband SAR Using an Adaptive Line Enhancer," *IEEE Geoscience and Remote Sensing Letters* **7**(4), 694–698 (2010).

[14] Le, C., Hensley, S., and Chapin, E., "Adaptive filtering of RFI in wideband SAR signals," in [*Seventh Airborne Geoscience Workshop*], (1998).

[15] Golden Jr, A., Werness, S. A., Stuff, M. A., DeGraaf, S. R., and Sullivan Jr, R. C., "Radio frequency interference removal in a VHF/UHF deramp SAR," in [*SPIE's 1995 Symposium on OE/Aerospace Sensing and Dual Use Photonics*], 84–95, International Society for Optics and Photonics (1995).

[16] Bickel, D. and Hensley, W. H., "Design, Theory, and Applications of Interferometric Synthetic Aperture Radar for Topographic Mapping," Tech. Rep. SAND96-1092 (1996).

[17] Bickel, D., "SAR Image Effects on Coherence and Coherence Estimation," Tech. Rep. SAND2014-0369 (2014).

[18] Preiss, M., Gray, D., and Stacy, N. J. S., "Detecting scene changes using synthetic aperture Radar interferometry," *IEEE Transactions on Geoscience and Remote Sensing* **44**(8), 2041–2054 (2006).

[19] Jakowatz, C. V., [*Spotlight-Mode Synthetic Aperture Radar: A Signal Processing Approach*], Springer (Jan. 1996).

[20] Doerry, A. W., "Collecting and processing data for high quality CCD images," tech. rep. (2007).

[21] Hanssen, R. and Bamler, R., "Evaluation of interpolation kernels for SAR interferometry," *IEEE Transactions on Geoscience and Remote Sensing* **37**, 318–321 (Jan. 1999).

[22] Just, D. and Bamler, R., "Phase statistics of interferograms with applications to synthetic aperture radar," *Applied Optics* **33**, 4361–4368 (July 1994).

[23] Buckreuss, S. and Horn, R., "E-SAR P-band SAR subsystem design and RF-interference suppression," in [*Geoscience and Remote Sensing Symposium Proceedings, 1998. IGARSS '98. 1998 IEEE International*], **1**, 466–468 vol.1 (July 1998).

[24] Doerry, A. W., Dickey, F. M., and Romero, L. A., "Windowing functions for SAR data with spectral gaps," **5095**, 54–65 (2003).